

## Spin relaxation in GaAs/Al<sub>x</sub>Ga<sub>1-x</sub>As quantum wells

A. Malinowski, R. S. Britton, T. Grevatt, and R. T. Harley

*Department of Physics and Astronomy, University of Southampton, Southampton SO17 1BJ, United Kingdom*

D. A. Ritchie and M. Y. Simmons

*Semiconductor Physics, Cavendish Laboratory, Madingley Road, Cambridge CB3 0HE, United Kingdom*

(Received 22 February 1999; revised manuscript received 9 November 1999)

Spin dynamics of photoexcited carriers in GaAs/Al<sub>x</sub>Ga<sub>1-x</sub>As quantum wells have been investigated in a wafer containing twelve different single quantum wells, allowing full investigation of well-width and temperature dependences with minimal accidental variations due to growth conditions. The behavior at low temperatures is dominated by excitonic effects, confirming results described in detail by others. Between 50 and 90 K there is a transition from excitonic to free-carrier-dominated behavior; both the temperature and time scale of the transition are in excellent agreement with a theoretical model for exciton dissociation. Above 90 K we find two-component spin decays consisting of an unresolved component (faster than 2 ps) associated with exciton dissociation and hole spin-relaxation and a longer-lived component that yields the electron spin-relaxation time. In the free-carrier regime, the electron spin-relaxation rate in wide wells follows that for bulk GaAs, which varies approximately as  $T^2$ . For narrow wells the rate is approximately independent of temperature and varies quadratically with confinement energy. This behavior is consistent with dominance of the D'yakonov-Perel mechanism of electron-spin relaxation and the expected behavior of the electron mobility. The data show evidence of the influence of electron scattering by interface roughness.

### I. INTRODUCTION

The understanding and control of spin relaxation of electrons, holes, and excitons in quantum wells are interesting because of the variety of competing mechanisms and because of potential applications such as optical switching<sup>1,2</sup> and polarization control in vertical cavity surface emitting lasers (VCSEL's),<sup>3</sup> where picosecond spin relaxation is desirable, and in spin electronics<sup>4,5</sup> and quantum computing,<sup>6</sup> where long spin-relaxation times are required. In this paper we describe time-resolved pump-probe measurements of spin-relaxation and photocarrier population dynamics in undoped GaAs/Al<sub>x</sub>Ga<sub>1-x</sub>As quantum wells. Previous experimental work has concentrated mainly on the low-temperature regime ( $T \leq 50$  K) where excitonic effects are dominant.<sup>7-12</sup> Here we are concerned principally with the transition from this low-temperature excitonic regime to the high-temperature regime where free-electron and hole spin relaxation is important and with temperature and well-width dependences in the high-temperature regime. Our results for the low-temperature regime are consistent with previous investigations.

Spin relaxation is strongly influenced by momentum scattering, which may vary unpredictably between samples. It is therefore useful to look at groups of samples with similar growth characteristics. In previous work<sup>13</sup> we reported trends in the electron spin-relaxation rate with confinement energy *at room temperature* in a group of samples that were grown sequentially in the same molecular beam epitaxy (MBE) machine and assessed the variation displayed by samples from a variety of other sources. Tackeuchi, Nishikawa, and Wada<sup>14</sup> have measured electron-spin-relaxation times at room temperature in samples containing single quantum wells whose thickness varied across the sample, allowing examination of a small range of well widths without complications from accidental differences between samples. Here we have exam-

ined quantum wells of thickness from 3 to 20 nm contained within a single wafer and have measured the temperature dependence of the spin relaxation in the free-carrier regime. The results thus cover a significantly wider range than previous work and should be free of sample-sample variations. This is crucial in identifying the dominant spin-relaxation mechanism. In addition we reveal clearly the transition from excitonic low-temperature spin-relaxation- to free-carrier-dominated relaxation at high temperatures. The data for free electrons demonstrate strong enhancement of spin relaxation by quantum confinement.

### II. EXPERIMENTAL METHODS

The sample was grown by MBE on a semi-insulating [100] substrate and consisted of a set of intrinsic GaAs/Al<sub>0.35</sub>Ga<sub>0.65</sub>As single quantum wells of thickness varying from 3 to 30 nm separated by 15-nm barriers with the wider wells nearer the substrate and a 50-nm GaAs capping layer. Between the substrate and the quantum wells there was a 1- $\mu$ m GaAs buffer followed by a 20-period, 2.8-nm GaAs/Al<sub>x</sub>Ga<sub>1-x</sub>As superlattice. It has been characterized by cw spectroscopy, being sample *A* in Ref. 15. The photoluminescence widths are comparable to the Stokes shifts, which vary from 5.2 meV in the 4-nm well to 0.02 meV in the 30-nm well. The interface roughness is found<sup>15</sup> to be on a length scale less than the exciton Bohr radius  $a_B \sim 13$  nm.

The population and spin dynamics were investigated by measurements of the intensity and polarization azimuth rotation of a 2-ps optical probe pulse after reflection from the sample following stimulation of the sample by a circularly polarized pump pulse. A schematic of the apparatus is shown in Fig. 1. Pump and (delayed) probe pulses were of the same wavelength, derived from the same mode-locked tuneable Ti:sapphire laser, giving 2-ps pulses with an 80-MHz repeti-

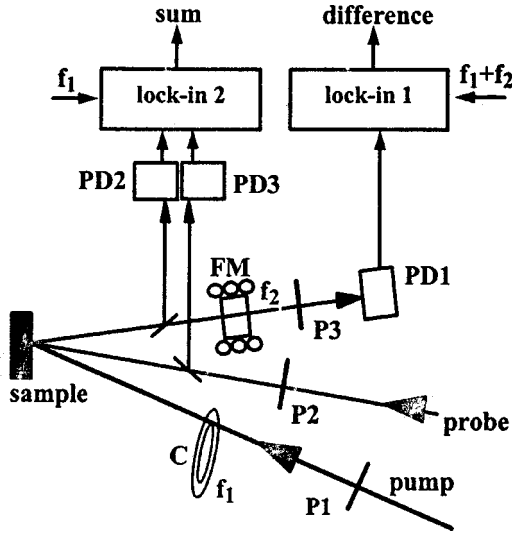


FIG. 1. Experimental setup. Pump and probe beams produced by same mode-locked Ti:sapphire laser.  $C$  is the mechanical chopper with frequency  $f_1 = 660$  Hz, FM is the Faraday modulator with frequency  $f_2 = 545$  Hz;  $P1-P3$  are polarizers;  $PD1-PD3$  are  $p-i-n$  photodetectors.

tion frequency. They were tuned to the heavy-hole exciton resonance of the quantum well under investigation. The pump beam was circularly polarized (polarizer  $P1$ ) and mechanically chopped at  $\sim 660$  Hz ( $f_1$ ), while the probe was linearly polarized ( $P2$ ). The average powers of pump and probe beams were, respectively, 500 and 50  $\mu$ W, and they were focused onto the sample with spot sizes 50 and 40  $\mu$ m at  $5^\circ$  and  $2^\circ$  to normal incidence. The estimated pump excitation density used in most of the measurements presented here was  $10^{10}$  cm<sup>-2</sup>/pulse; as described in Sec. IV, the density dependence of spin-relaxation rates was observed to be very weak. The degree of circular polarization of the pump light was greater than 0.95, which implies a similar initial degree of photocarrier spin polarization for excitation at the heavy-hole exciton.

After reflection from the sample the probe beam passed to a silicon  $p-i-n$  detector (PD1) via a Faraday modulator (FM) and a linear polarizer ( $P3$ ) crossed with the  $P2$  polarizer. The Faraday modulator produced  $\sim \pm 10^{-2}$  rad of azimuth rotation at 545 Hz ( $f_2$ ). The output of detector PD1 was passed to lock-in amplifier 1, which was referenced at frequency  $f_1 + f_2$ , thus giving an output proportional to changes in probe azimuth induced by the pump. This will be referred to as the *difference* signal and arises from different optical responses experienced by the left and right circularly polarized components of the linearly polarized probe. The dominant process causing such circular birefringence is the unequal phase-space filling due to imbalance of population of opposite carrier spins induced by the circularly polarized pump.<sup>16</sup> The difference signal contains information on spin relaxation as well as on population dynamics.

To obtain a measure of the total carrier density, independent of differences of population of the spin states, detectors PD2 and PD3 sensed the intensity of the reflected and incident probe beams, respectively. Their two signals were matched and subtracted in lock-in amplifier 2, referenced to the chopping frequency  $f_1$ , giving output sensitive to the

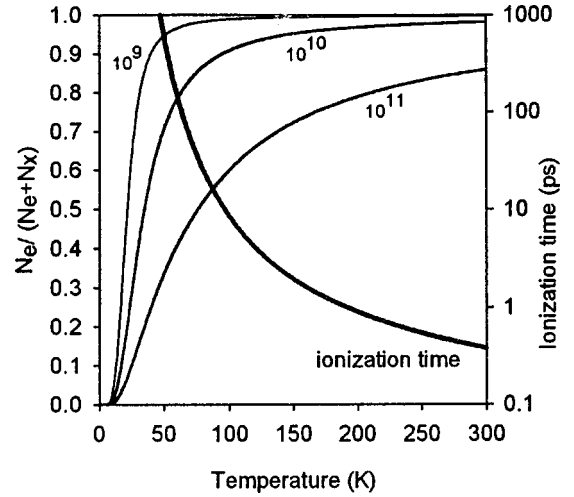


FIG. 2. Calculated thermal equilibrium carrier concentration ratio and exciton ionization time in an undoped 10-nm quantum well.  $N_e$  and  $N_x$  are the electron and exciton concentrations and are displayed for excitation densities of  $10^9$ ,  $10^{10}$ , and  $10^{11}$  cm<sup>-2</sup>. Note the logarithmic scale for the ionization time.

pump-induced change in the reflectivity of the sample. This will be referred to as the *sum* signal and is also dominated by the phase-space-filling effect of the pump-induced carrier population.<sup>16</sup> Compared to separate measurements of the reflectivity of the two circularly polarized components<sup>13</sup> of the probe, the azimuth rotation gives excellent signal-to-noise ratio and enables extraction of pure spin relaxation from the ratio of difference-to-sum signals. The reflection geometry avoids degradation of the quantum-well quality associated with removal of the substrate. A disadvantage is that only qualitative comparisons can be made between the magnitudes of signals recorded at different temperatures (see Sec. IV and Fig. 3) due to the complexity of the wavelength dependence of the signals, which is associated with the complexity of the linear reflectivity of multilayer samples.

### III. CARRIER CONCENTRATIONS

Interpretation of temperature-dependent measurements requires knowledge of the ratio of free-carrier pairs to excitons in the photoexcited population. Our experiments involve resonant generation of excitons, so any free carriers must be formed by exciton ionization and can only dominate the observations at delays greater than the ionization time and at temperatures where thermal equilibrium favors exciton dissociation.

We have calculated the thermal equilibrium proportion of free electrons in the population as a function of excitation density and temperature using the approach given in Ref. 17, and the results for a 10-nm GaAs quantum well (QW) are shown in Fig. 2. Free electrons (and holes) dominate at low excitation densities and high temperatures. At the excitation densities used in our experiments ( $N \sim 10^{10}$  cm<sup>-2</sup>/pulse), free carriers will be dominant at equilibrium down to about 40 K. In fact, since the calculation neglects screening, which will tend to reduce the number of possible exciton states at high densities, it probably underestimates the equilibrium proportion of free carriers for a particular temperature and excitation density.

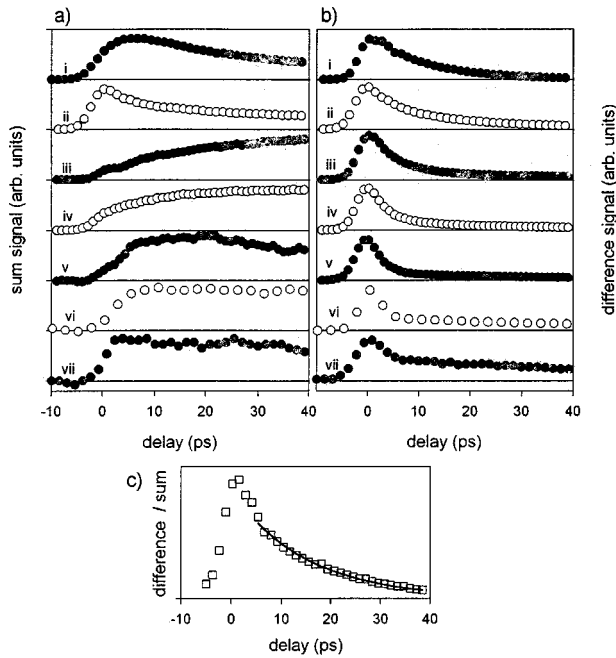


FIG. 3. Normalized plots of (a) sum and (b) difference signals from the 10-nm quantum well at a variety of temperatures: *i*, 5.5 K; *ii*, 40 K; *iii*, 55 K; *iv*, 70 K; *v*, 85 K; *vi*, 130 K; *vii*, 200 K. For temperatures greater than 40 K a nonzero background has been subtracted from the sum signals. (c) shows the ratio of the difference and sum signals at 5.5 K. The solid curve is a single exponential fit to the decay.

Figure 2 also shows the calculated exciton ionization time as a function of temperature, again using the approach given in Ref. 17. Ionization is assumed to proceed predominantly via exciton-LO-phonon interaction. At room temperature the calculated ionization time is  $\sim 400$  fs, close to measured values for similar quantum wells;<sup>18</sup> it is about 10 ps at 100 K and increases very rapidly with falling temperature, reaching 100 ps at about 50 K.

The conclusion is that in our experiment below about 90 K the carrier populations will not be in thermal equilibrium during spin relaxation, which typically takes 10–100 ps. Above this temperature, ionization is fast enough for the behavior to be dominated by free electrons and holes. Below 50 K, ionization is so slow that it can be neglected, and the spin relaxation, for resonant generation, will be purely excitonic. Between 50 and 90 K we expect a transition region where thermal equilibrium, in which free carriers predominate, is established on a comparable time scale to spin relaxation. This transition region will not be significantly dependent on the quantum-well width and will be characterized by a buildup of effects associated with free carriers on the time scale of the ionization time (Fig. 2). (Neglect of acoustic phonons may result in an overestimate of the ionization time at low temperatures, but this will not significantly change the conclusions.)

#### IV. RESULTS AND DISCUSSION

Figures 3(a) and 3(b) show normalized sum and difference signals from a 10-nm well at various temperatures. The sum signal indicates the pump-induced change of reflectivity and the difference the probe polarization rotation. Note that

the reflection-measurement technique allows only a qualitative comparison of the magnitudes of signals between data taken at different temperatures (see Sec. II). Qualitatively similar data were obtained from the wells of different thickness in this sample, and we have found similar behavior in a variety of other samples grown independently.<sup>19</sup> In addition, in the present sample we have investigated the dependence on estimated pump excitation density between  $10^9$  and  $3 \times 10^{10} \text{ cm}^{-2}$  at temperatures of 5, 55, 100, and 300 K and do not find significant variations. In previously reported experiments at room temperature we have demonstrated that electron-spin relaxation is unaffected by a background photoexcited, unpolarized electron-hole concentration  $\sim 10^{11} \text{ cm}^{-2}$ .<sup>13</sup>

At low temperature (5.5 K) the sum and difference signals can be interpreted in terms of heavy-hole-exciton population dynamics in the low-density, noninteracting regime.<sup>7,8</sup> The sum shows a rapid fall from its initial peak over the first  $\sim 20$  ps followed by a longer decay, lasting several hundred picoseconds. This is similar to results of low-temperature luminescence experiments.<sup>8</sup> The fast initial decay may be due to thermalization of excitons to nonradiative large- $k$  states outside the absorption linewidth and to exciton recombination<sup>8</sup> and there may also be a contribution from exciton-exciton exchange interaction.<sup>11</sup> The longer decay is assigned to recombination of the thermalized exciton population, which slows down once most excitons have moved out of radiatively coupled states. At 5.5 K the initial rise of the sum signal corresponds to the buildup of carrier population during the finite duration of the pump pulse, which is then followed by a decay on a time scale that is long compared to the pulse width. The difference signal shows a markedly faster overall decay as a result of spin relaxation as well as decay of the population. The ratio of the difference and sum signals [Fig. 3(c)] yields a spin-relaxation time of  $\sim 20$  ps, consistent with the spin relaxation due to the exciton exchange mechanism.<sup>7,8</sup> The more rapid rise of the difference signal compared with the sum results from convolution of the pulse shape with the more rapid decay. At 40 K, the decays are qualitatively similar to those at 5.5 K; a two-component response is still visible in the sum signal but with faster initial decay, and the difference shows a more nearly single exponential decay. Again the rapid rising edges of the signals at 40 K relative to the sum at 5.5 K is associated with finite pulse width. We have not reinvestigated the exciton-dominated regime (i.e.,  $T \leq 40$  K) in detail for this sample, but the results are at least qualitatively similar to those reported elsewhere.<sup>8,11,16</sup>

At 55 K new behavior is observed (Fig. 3); the sum signal now has a very long-lived component, and a background ( $\sim 20\%$  of the total signal) appears at negative delay (suppressed in Fig. 3), which corresponds to carrier recombination time comparable to the interpulse spacing of the laser.<sup>20</sup> Immediately following the pump pulse the sum signal shows a weak maximum that is followed by a gradual increase with rise time of about 22 ps approaching a new, nonzero value. At 70 K, the initial peak is barely discernible as an abrupt rising edge and this is followed by a slower increase with rise time of about 10 ps. The background has increased to  $\sim 30\%$  of the total signal. To interpret this behavior we note that at these temperatures free carriers are expected to bleach

the absorption (and therefore change the reflectivity) approximately twice as effectively as excitons.<sup>21</sup> Thus the initial peak followed by a gradual rise in the sum signal to a nonzero level represents the initial generation followed by ionization of excitons to free carriers, which then have lifetimes of many nanoseconds.<sup>20</sup> The observed rise times are within a factor of 4 of the ionization times predicted in Sec. III (see Fig. 2), which constitutes excellent agreement considering the very strong predicted temperature dependence of the ionization time.

Due to the complicated nature of the carrier dynamics between 50 and 90 K, we cannot unambiguously combine sum and difference data to extract the spin-relaxation rate. As we move to higher temperatures the transition to free carriers becomes faster than our pulse duration, and we observe a simple resolution-limited step in the sum signal. The background level on the sum continues to increase with temperature, representing  $\sim 80\%$  of the total signal at 200 K. At temperatures above about 85 K the difference response divides into an initial spike on the time scale of the pulse duration and a long-lived exponentially decaying component. We interpret this in terms of exciton dissociation and free-carrier spin relaxation.

Free-hole spin relaxation in bulk GaAs is fast (a few picoseconds), even at low temperature, due to the  $p$ -orbital character of the valence bands, which leads to spin-orbit admixture of the heavy- ( $m_j = \pm \frac{3}{2}$ ) and light-hole ( $m_j = \pm \frac{1}{2}$ ) states. In quantum wells, the heavy-hole–light-hole degeneracy is lifted, strongly reducing the relaxation rate at  $k = 0$ ; hole-spin-relaxation times approaching 1 ns have been recorded at low temperature in GaAs QW.<sup>22,23</sup> In higher  $k$  states there is progressive admixture of heavy- and light-hole bands that leads to a very strong dependence of the spin-relaxation rate on kinetic energy and hence temperature; the observed rate is less than 5 ps for  $T > 50$  K.<sup>22</sup> It has also been observed that hole-spin relaxation takes place on a subpicosecond time scale in type-II multiple quantum wells (MQW's) at room temperature.<sup>24</sup> We therefore expect that in our samples hole-spin relaxation will be faster than our experimental resolution ( $\sim 2$  ps) at temperatures  $T > 90$  K. Consequently the new long-lived component must be associated with free-electron-spin relaxation while the initial spike combines the effects of free-hole-spin relaxation and exciton ionization, which are expected to occur on a time scale that is too short to be resolved. The long-lived component of the difference signal is well described by a single exponential decay, which is an accurate measure of the pure electron-spin-relaxation time since the sum signal is effectively constant during the decay.

We investigated the electron-spin-relaxation rate for each quantum well in the sample as a function of temperature in the range 90–300 K. Figure 4 shows a representative selection of the data. Also included is representative data for  $4 \times 10^{16} \text{ cm}^{-3}$   $p$ -doped bulk GaAs.<sup>25</sup> Although the experimental scatter is quite large, several conclusions can be drawn from the results. The two narrowest wells show little or no variation in spin-relaxation rate over the entire temperature range. The rate for the 15-nm well is initially constant at low temperatures but tends to increase at higher temperatures, approximating a  $T^2$  variation above 200 K (see line in Fig. 4). For the 20-nm well the rate increases as  $T^2$  over the

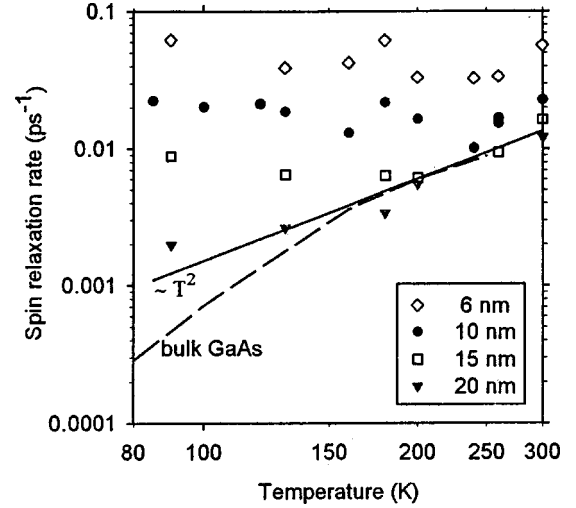


FIG. 4. Electron-spin-relaxation rate as a function of temperature in GaAs/Al<sub>x</sub>Ga<sub>1-x</sub>As quantum wells of a variety of widths. The solid line represents a quadratic dependence of relaxation rate on temperature. The dashed curve is data on electron-spin relaxation in bulk GaAs from Maruschak *et al.* (as reproduced in Ref. 25).

whole temperature range. The rates for the two wider wells are essentially the same above 200 K.

This behavior is consistent with predictions for the D'Yakonov-Kachorovski<sup>26</sup> and D'Yakonov-Perel<sup>27</sup> (DP) mechanisms for electron-spin relaxation in quantum-well and bulk semiconductors. For the electron-momentum relaxation time  $\tau_p$  and quantum confinement energy  $E_{1e}$ , they predict that the spin-relaxation rate will scale as  $\tau_p T^3$  in bulk material and in quantum wells, where  $E_{1e} < k_B T$  (i.e., wide wells at high temperatures), and as  $\tau_p T E_{1e}^2$  in quantum wells, where  $E_{1e} > k_B T$  (i.e., narrow wells at low temperatures).

We do not have data on  $\tau_p$  in this sample, but over much of the temperature range 90–300 K we expect  $\tau_p$  to be similar in both bulk and quantum-well material; phonon scattering is likely to be the dominant source of scattering, with lesser contributions from impurities, barrier alloy,<sup>28</sup> and interface roughness.<sup>29</sup> Therefore the ratio of bulk to quantum-well spin relaxation rates should vary as  $T^2$ , as is observed experimentally above about 160 K. The constancy of relaxation rates in narrow wells indicates a  $T^{-1}$  dependence of  $\tau_p$  (and hence of electron mobility). This is weaker than in the best high-mobility heterojunction, but consistent with significant contributions to the scattering in addition to that of phonons. At lower temperatures impurity and defect scattering will become more significant and  $\tau_p$  will therefore be different in bulk and quantum wells, giving a bulk-to-quantum-well ratio which deviates from  $T^2$  temperature dependence. This is seen in Fig. 4 below 150 K where the quantum-well rates, if anything, increase slightly, whereas the bulk curve falls below the  $T^2$  line. At low temperatures, there are significant differences between spin-relaxation rates in different bulk samples,<sup>25</sup> consistent with variations in mobility.

The alternative spin-relaxation mechanisms due to Elliott and Yaffet<sup>30</sup> (EY) and to Bir, Aharonov, and Pikus<sup>31</sup> (BAP) each predict relaxation rates that are several orders of magnitude too low to explain the observed values. They also predict incorrect temperature and well-width dependences.

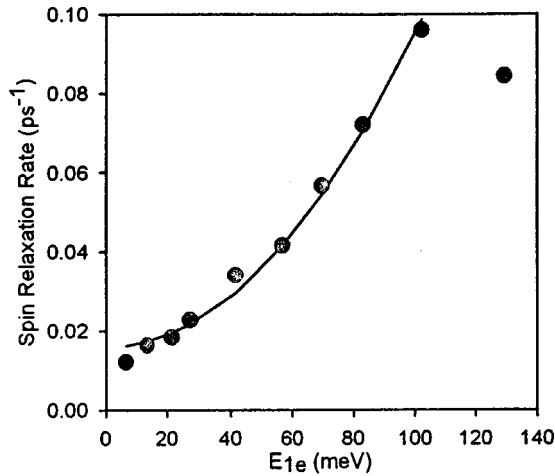


FIG. 5. Electron-spin relaxation as a function of confinement energy in GaAs/Al<sub>x</sub>Ga<sub>1-x</sub>As quantum wells ( $T=300$  K). The solid curve is a best fit to the data of the form  $\tau_s^{-1} = a + bE_{1e}^2$ .

The rate due to the EY mechanism scales as  $\tau_p^{-1}T^2$  in both bulk<sup>25,32</sup> and quantum-well material,<sup>33</sup> and to match this to the observed data we would require the electron mobility in the sample to increase unrealistically with temperature. The BAP mechanism is not dependent on the electron mobility and is expected to have a relatively weak dependence on temperature in both quantum well and bulk.<sup>34,32</sup> Therefore the BAP mechanism appears to be inconsistent with the observed qualitatively different behavior in narrow and wide wells.

We made more precise measurements of the electron-spin-relaxation rate at 300 K for each quantum well in the sample. Figure 5 shows the data plotted against the electron confinement energy  $E_{1e}$ . The confinement energies were determined using low-temperature luminescence spectroscopy. For low confinement energies ( $E_{1e} < k_B T$ ) we see values of  $\tau_s^{-1}$  close to the bulk value  $1.3 \times 10^{10} \text{ s}^{-1}$  (Ref. 25). As  $E_{1e}$  rises, we see an additional term in the relaxation rate with quadratic dependence on confinement energy as predicted for the DP mechanism in quantum wells with constant momentum relaxation time  $\tau_p$ . The solid curve is a fit to the data of the form  $\tau_s^{-1} = a + bE_{1e}^2$ . For the largest value of confinement energy (well width 3 nm) the relaxation rate turns downwards, deviating strongly from the quadratic dependence, indicating additional momentum scattering. We have previously observed similar behavior with a quadratic dependence on confinement energy but downward deviation for 2.5-nm wells in a series of MQW samples.<sup>13</sup> The fact that the effect appears also in the present sample gives it added significance.

To explain the observed downturn of the spin-relaxation rate requires a very strongly well-width-dependent scattering mechanism. Interface roughness scattering should have a sufficiently strong well-width dependence. Sakaki *et al.*<sup>29</sup> calculated an  $L_z^{-6}$  dependence of electron mobility on well width due to this mechanism in a GaAs/AlAs QW. Hillmer, Forched, and Tu<sup>28</sup> have calculated the ambipolar mobility in GaAs/Al<sub>x</sub>Ga<sub>1-x</sub>As wells; they do not obtain a simple power-law dependence, but the calculated well-width dependence is strong enough to account for the low relaxation rate of our narrowest well. Scattering by interface roughness is most

efficient when the lateral scale of the roughness is of the same order as the wavelength of the electron, and therefore is strongly dependent on the growth conditions of the sample. This is consistent with the fact that some but not all sets of samples show a downturn of spin-relaxation rate for the narrowest wells. In this sample the scale of the interface roughness is less than 13 nm,<sup>15</sup> which should give efficient scattering of electrons with a thermal in-plane wavelength at 300 K. In contrast, scattering due to acoustic phonons is only inversely proportional to well width, which is clearly too weak a dependence to produce the observed results in narrow wells.<sup>28</sup> Barrier alloy scattering due to penetration of electron wave functions into the barrier material is well-width dependent but does not become strong enough to reduce the mobility below its bulk value until a well width of about 2 nm is reached.<sup>28</sup>

## V. SUMMARY AND CONCLUSIONS

We have investigated spin relaxation of photoexcited carriers in GaAs/Al<sub>x</sub>Ga<sub>1-x</sub>As quantum wells as a function of temperature and quantum-well width. At low temperatures ( $T \leq 50$  K) the spin relaxation is dominated by excitonic effects, and the rate is enhanced compared to free carriers by electron-hole exchange interaction, consistent with previous investigations.<sup>7,8</sup> At temperatures between 50 and 90 K there is a transition from excitonic to free-carrier-dominated behavior that is well described by a model for thermal exciton dissociation.<sup>17</sup> Thermal equilibrium conditions for exciton dissociation would favor free carriers at considerably lower temperatures, but for resonant exciton generation the transition is only observed when the exciton ionization rate, which varies very rapidly with temperature, becomes comparable to the spin relaxation rates. In the range 90–300 K the data give the free-electron-spin-relaxation rate. For narrow wells and low temperatures ( $kT < E_{1e}$ ), this rate is independent of temperature, whereas for wider wells and higher temperatures ( $kT > E_{1e}$ ) the rate becomes approximately proportional to  $T^2$  and is close to that of bulk GaAs. This behavior is fully consistent with the D'Yakonov-Perel mechanism of electron-spin-relaxation.

The results emphasize the manner in which quantum confinement dramatically enhances the spin-relaxation rate for electrons compared to bulk GaAs. In our sample at room temperature the enhancement appears to be limited by onset of interface roughness scattering. This might be removed and greater enhancement achieved by use of interrupted growth techniques that give roughness with a greater length scale. The extreme enhancement would occur for electrons in weakly  $n$ -type material at liquid-helium temperatures where exciton effects are screened out. On the one hand, measurements in  $\delta$ -doped double heterostructures,<sup>34</sup> type-II quantum wells,<sup>35</sup> and more recently<sup>4</sup> on bulk GaAs have indicated spin-relaxation times in excess of 25 ns, presumably limited by the Elliot-Yafet processes. But, on the other hand, our data suggest spin-relaxation times of electrons in good-quality quantum wells will be in the range 50–500 ps, still determined by the D'Yakonov-Perel mechanism. Poorer quality wells, with lower mobilities, will have longer spin-relaxation times. These findings are relevant to the design of fast nonlinear optical spin switches and also to spin electronics where long relaxation times are desirable.

- <sup>1</sup>Y. Nishikawa, A. Tackeuchi, S. Nakamura, S. Muto, and N. Yokoyama, *Appl. Phys. Lett.* **66**, 839 (1995).
- <sup>2</sup>J. T. Hyland, G. T. Kennedy, A. Miller, and C. C. Button, *IEEE Photonics Technol. Lett.* **10**, 1419 (1998).
- <sup>3</sup>M. San Miguel, Q. Feng, and J. V. Moloney, *Phys. Rev. A* **52**, 1728 (1995).
- <sup>4</sup>J. M. Kikkawa and D. D. Awschalom, *Phys. Rev. Lett.* **80**, 4313 (1998).
- <sup>5</sup>G. Prinz, *Phys. Today* **48** (4), 58 (1995).
- <sup>6</sup>B. E. Kane, *Nature (London)* **393**, 133 (1998).
- <sup>7</sup>M. Z. Maialle, E. A. de Andrada e Silva, and L. J. Sham, *Phys. Rev. B* **47**, 15 776 (1993).
- <sup>8</sup>A. Vinattieri, Jagdeep Shah, T. C. Damen, D. S. Kim, L. N. Pfeiffer, M. Z. Maialle, and L. J. Sham, *Phys. Rev. B* **50**, 10 868 (1994).
- <sup>9</sup>R. T. Harley and M. J. Snelling, *Phys. Rev. B* **53**, 9561 (1996).
- <sup>10</sup>R. E. Worsley, N. J. Traynor, T. Grevatt, and R. T. Harley, *Phys. Rev. Lett.* **76**, 3224 (1996).
- <sup>11</sup>T. Amand, D. Robart, X. Marie, M. Brousseau, P. Le Jeune, and J. Barrau, *Phys. Rev. B* **55**, 9880 (1997); P. Le Jeune, X. Marie, T. Amand, F. Romstad, F. Perez, J. Barrau, and M. Brousseau, *ibid.* **58**, 4853 (1998).
- <sup>12</sup>J. Shah, *Ultrafast Spectroscopy of Semiconductors and Semiconductor Nanostructures*, Springer Series in Solid State Science Vol. 115 (Springer, Berlin, 1996), and references cited therein.
- <sup>13</sup>R. S. Britton, T. Grevatt, A. Malinowski, R. T. Harley, P. Perozzo, A. R. Cameron, and A. Miller, *Appl. Phys. Lett.* **73**, 2140 (1998).
- <sup>14</sup>A. Tackeuchi, Y. Nishikawa, and O. Wada, *Appl. Phys. Lett.* **68**, 797 (1996).
- <sup>15</sup>N. Garro, L. Pugh, R. T. Phillips, V. Drouot, M. Y. Simmons, B. Kardynal, and D. A. Ritchie, *Phys. Rev. B* **55**, 13 752 (1997).
- <sup>16</sup>M. J. Snelling, P. Perozzo, D. C. Hutchings, I. Galbraith, and A. Miller, *Phys. Rev. B* **49**, 17 160 (1994).
- <sup>17</sup>D. S. Chemla, D. A. B. Miller, P. W. Smith, A. C. Gossard, and W. Wiegmann, *IEEE J. Quantum Electron.* **20**, 265 (1984).
- <sup>18</sup>W. H. Knox, R. L. Fork, M. C. Downer, D. A. B. Miller, D. S. Chemla, C. V. Shank, A. C. Gossard, and W. Wiegmann, *Phys. Rev. Lett.* **54**, 1306 (1985).
- <sup>19</sup>T. Grevatt, Ph.D. thesis, University of Southampton (1996).
- <sup>20</sup>J. Feldmann, G. Peter, E. O. Gobel, P. Dawson, K. Moore, C. Foxon, and R. J. Elliott, *Phys. Rev. Lett.* **59**, 2337 (1987).
- <sup>21</sup>S. Schmitt-Rink, D. S. Chemla, and D. A. B. Miller, *Phys. Rev. B* **32**, 6601 (1985).
- <sup>22</sup>B. Baylac, T. Amand, X. Marie, B. Dareys, M. Brousseau, G. Bacquet, and V. Thierry-Mieg, *Solid State Commun.* **93**, 57 (1995).
- <sup>23</sup>R. T. Harley, in *Coherent Optical Interactions in Semiconductors*, edited by R. T. Phillips (Plenum, New York, 1994), p. 91.
- <sup>24</sup>T. Kawazoe, T. Mishina, and Y. Masumoto, *Jpn. J. Appl. Phys., Part 2* **32**, L1756 (1993).
- <sup>25</sup>*Optical Orientation*, edited by F. Meier and B. P. Zakharchenya (North-Holland, Amsterdam, 1984).
- <sup>26</sup>M. I. D'Yakonov and V. Yu. Kachorovski, *Fiz. Tekh. Poluprodn.* **20**, 178 (1986) [*Sov. Phys. Semicond.* **20**, 110 (1986)].
- <sup>27</sup>M. I. D'Yakonov and V. I. Perel, *Fiz. Tverd. Tela (Leningrad)* **13**, 3581 (1971) [*Sov. Phys. Solid State* **13**, 3023 (1972)].
- <sup>28</sup>H. Hillmer, A. Forchel, and C. W. Tu, *J. Phys.: Condens. Matter* **5**, 5563 (1993).
- <sup>29</sup>H. Sakaki, T. Noda, K. Hirakawa, M. Tanaka, and T. Matsusue, *Appl. Phys. Lett.* **51**, 1934 (1987).
- <sup>30</sup>R. J. Elliott, *Phys. Rev.* **96**, 266 (1954).
- <sup>31</sup>G. L. Bir, A. G. Aronov, and G. E. Pikus, *Zh. Eksp. Teor. Fiz.* **69**, 1382 (1975) [*Sov. Phys. JETP* **42**, 705 (1975)].
- <sup>32</sup>G. Fishman and G. Lampel, *Phys. Rev. B* **16**, 820 (1977).
- <sup>33</sup>A. D. Margulis and V. I. Margulis, *Fiz. Tekh. Poluprovodn.* **18**, 493 (1984) [*Sov. Phys. Semicond.* **18**, 305 (1984)].
- <sup>34</sup>J. Wagner, H. Schneider, D. Richards, A. Fischer, and K. Ploog, *Phys. Rev. B* **47**, 4786 (1993).
- <sup>35</sup>W. A. J. A. van der Poel, A. L. G. J. Severens, H. W. van Kesteren, and C. T. Foxon, *Superlattices Microstruct.* **5**, 115 (1989).